ACS APPLIED MATERIALS & INTERFACES

Surfaces, Interfaces, and Applications

High-Fidelity Hydrogel Thin-Films Processed from Deep Eutectic Solvents

David Delgado, Daniel Rudolf King, KUNPENG CUI, Jian Ping Gong, and Kenneth R Shull

ACS Appl. Mater. Interfaces, **Just Accepted Manuscript** • DOI: 10.1021/acsami.0c09618 • Publication Date (Web): 21 Aug 2020

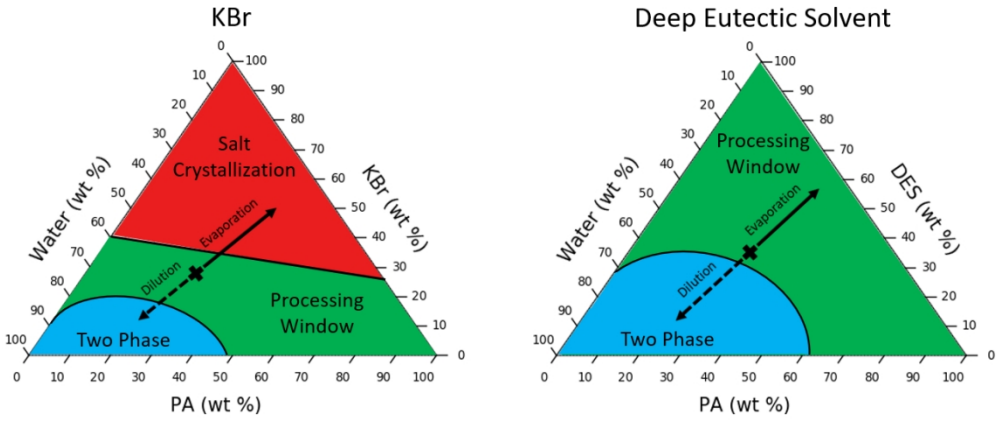

TOC image

345x145mm (96 x 96 DPI)

High-Fidelity Hydrogel Thin-Films Processed from Deep Eutectic Solvents

E-mail:

David E. Delgado[§], Daniel R. King[†ς*], Kunpeng Cui[‖], Jian Ping Gong[†ς‖], and Kenneth R. Shull[§*]

[§]Department of Materials Science and Engineering, Northwestern University, Evanston, IL 60208, United States

[†]Faculty of Advanced Life Science, [ς]Global Station for Soft Matter, Global Institution for Collaborative Research, [‖]Institute for Chemical Reaction Design and Discovery, Hokkaido University, Sapporo 001-0021, Japan

[*] To whom correspondence should be addressed: k-shull@northwestern.edu, dking@mail.sci.hokudai.ac.jp

Abstract

Polyampholyte (PA) hydrogels are a fascinating class of soft materials that can exhibit high toughness while retaining self-healing characteristics. This behavior results from the random distribution of oppositely charged monomers along the polymer chains that form transient bonds with a range of bond strengths. PAs can be dissolved in aqueous salt solutions and then re-cast via immersion precipitation, making them particularly useful as surface coatings in biomedical applications. Moreover, this immersion precipitation technique allows these PA hydrogels to be fabricated into films

less than 100 nm. One critical challenge to this aqueous processing method is the re-crystallization of the salt upon water evaporation. Such re-crystallization can disrupt the hydrogel morphology especially in thin films. In this study, a deep eutectic solvent (DES) formed from urea and choline chloride was used to dissolve PAs made from p-styrenesulfonic acid sodium salt and 3-(methacryloylamino)propyl trimethylammonium chloride. This DES has a freezing point of 12°C, allowing it to remain stable and liquid-like at room temperatures. Thus, these PAs can be processed in DES solutions, without this issue of re-crystallization and with simple methods such as spin coating and dip coating. These methods allow these hydrogels to be used in thin (<100 nm) film coating applications. Finally, the complete miscibility of DES in water allows a wider range of 1 phase compositions and expands the processing window of these polyampholyte materials.

Introduction

Due to their tunable chemistries and ability to retain high amounts of water, hydrogels are applicable to many fields, ranging from soft robotics to sensors to biomaterials.[1–3] For use in artificial skin or blood vessel applications, hydrogel thin films are especially of interest. However, the inherently poor mechanical properties of traditional (e.g. single network polyacrylamide hydrogels) hydrogels renders these materials unsuitable for many thin-film applications.[4] Both new materials as well as new fabrication techniques are required to satisfy the requirements for biomaterials applications.

The mechanical properties of hydrogels for biomedical materials have significantly improved over the last two decades, due to the discovery of new toughening mechanisms[5]. One of the most influential advancements was "double network" (DN) hydrogels, where a stiff yet brittle sacrificial network is incorporated within a soft and stretchable network. Through this topology, the sacrificial bonds rupture first, dissipating energy and improving the overall strength and toughness of the gel.[6–8] One limitation of this approach, however, is that

the rupture of covalent bonds is irreversible, causing significant hysteresis and permanent softening after deformation of the gel.[9]

To overcome this problem, sacrificial networks based on reversible bonds such as van der Waals interactions, hydrogen bonds, and ionic bonds have been employed. These methods allow for recovery of hysteresis energy and self-healing capabilities. Polyampholyte hydrogels represent a specific type of reversibly bonded tough hydrogel, where anionic and cationic monomers exist along the same backbone.[10–13] Charge interactions in this system will either swell or deswell in aqueous solutions depending on the total monomer concentration at preparation, the salt content of the solution, and charge ratio.[14] Moreover, PA hydrogels synthesized by random copolymerization of oppositely charged ionic monomers form multiple ionic bonds with a wide distribution of strengths due to inter- and intra-chain complexation.This range of bond strengths allows the hydrogel to retain some of the robustness found in double-network gels while having the entire network be transient and thus self-healing.[14–16]

While significant progress has been made in increasing the mechanical properties of hydrogels, there has been limited effort to develop them into thin films. Films on the order of 30 microns have been made with traditional DN gels, and 100 microns with particle-based DN gels.[17,18] Recently, a new type of block-copolymer-based DN gel has been developed, which can be used to create films as thin as ~5 microns.[16,19] By contrast, polyampholyte gels are currently polymerized overnight as static, thick (mm) sheets, thus limiting their thin film applications (minimum thickness: ~300 microns). Thus, a significant advancement would be to leverage the transient nature of these PA hydrogels to dissolve existing bulk samples and re-cast them into 'high fidelity' films. By this we mean that films with desired thicknesses could be cast onto a wide variety of surfaces while accurately preserving the substrate morphology.

Polyelectrolyte complexes are similar to polyampholytes in that they form networks based on ionic interactions, but in this case charges are sequestered into separate polymer chains.

Upon combination in aqueous solutions, counter-ions are released, forming a complex due to the large gain in entropy.[20,21] These precipitates were once deemed unprocessable, however, it was discovered that the inclusion of salt partially dopes electrostatic bonds allowing the complex to swell with water.[22] In a certain range of salt concentrations, these complexes become viscoelastic fluids called "coacervates" that can be processed like a traditional polymer. Moreover, these coacervates can be immersed in a bath of pure water causing an osmotic gradient to rapidly extract salt ions and produce a rigid complex that could not be fabricated without the addition of salt. Such a process has been used to manufacture these charged complexes into rods, sheets, and water filtration membranes.[23,24]

As polyampholyte gels possess similar transient molecular bonds, it is a natural progression to apply these salt doping and rapid quenching ideas to these materials. One major challenge, however, is the re-crystallization of salt within the complex or polyampholytes if the solution is exposed for too long in ambient conditions and the water evaporates. Especially in thin film applications, this evaporation can lead to salt re-crystallization that can compromise the film morphology. Thus, it would be ideal to reconcile this salt processing method with ions that do not crystallize during typical processing conditions. Ionic liquids are one potential option to fill this role.

Many commonly employed ionic liquids, however, are expensive, toxic, and difficult to produce at scale.[25,26] Deep eutectic solvents are a sub-class of ionic liquids that have many of the same advantageous characteristics, most notably their existence as liquids at room temperature. These characteristics are due to a hydrogen donor acting as a neutral "complexing agent" with a H-bond accepting anionic species which forms a larger charged complex.[27] In contrast to ionic liquids, however, many deep eutectic solvents have been found to be generally more affordable, potentially biodegradable, and easier to produce in bulk.[14,28]

A common deep eutectic solvent that will be employed in this work consists of a mixture of urea and choline chloride, with respective melting temperatures of 301 °C and 133 °C. When mixed, however, at a (2 : 1) molar ratio respectively and heated to 80 °C, these molecules form

an eutectic with a freezing point of 12 °C.[27,29] Such a low freezing point allows this ion pair to remain liquid-like even in ambient conditions. Moreover, it has been shown that the viscosity of the deep eutectic solvent solution can be tuned through the simple inclusion of water.[30–32] Thus, investigating the interplay between urea/choline chloride, water, and polyampholytes represents a tantalizing opportunity to process these hydrogels in an efficient and scalable manner.

In the following work, we introduce a method to make thin films without salt crystallization issues based on polyampholytes composed of 3-(methacryloylamino)propyl trimethylammonium (MPTC) and p-styrenesulfonic acid sodium salt (NaSS), as shown in Figure 1a. We first quantify the phase behavior of the model polyampholyte (PA) in a deep eutectic solvent (DES) comprised of urea and choline chloride as shown in Figure 1b, and compare to the phase behavior in high concentrations of potassium bromide (KBr). At sufficiently high concentrations, one-phase viscous solutions can be achieved, and subsequently deployed to create thin films. Through this process, polyampholyte films down to ~70 nm can be created. The thin film morphologies resulting from aqueous DES solutions are next compared to those from aqueous KBr solutions. We see that the utilization of DES allows for the formation of high-fidelity thin films, with minimal roughness, in comparison to the KBr solution-based films which suffer from high roughness due to salt crystallization. Finally, the effects of the DES and water composition on the rheological properties are then studied. By combining preferential morphological and mechanical properties, these materials can be used to coat active and complex surfaces, such as the ball of a ball-and-socket hip joint through a simple dip-coating procedure. The methods introduced here will be important to the development of thin-film hydrogels for future biomaterials applications.

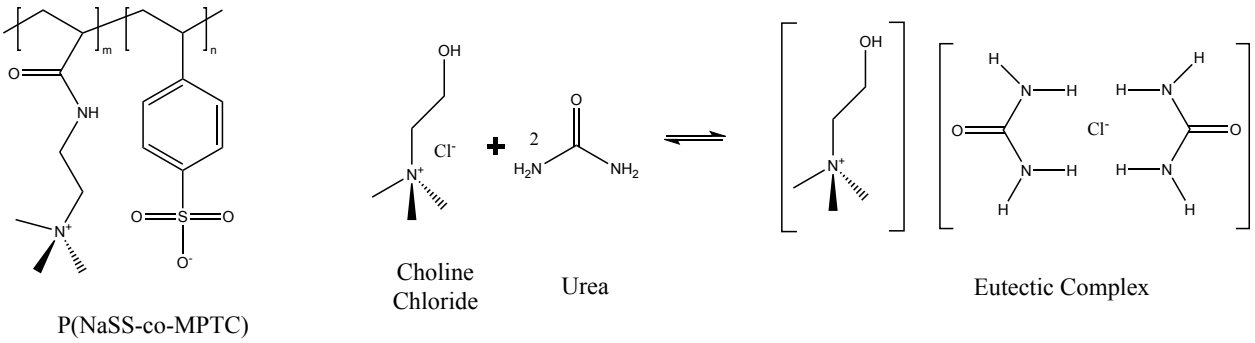

Figure 1: a) A polyampholyte formed from 3-(methacryloylamino)propyl trimethylammonium chloride and p-styrenesulfonic acid sodium salt. b) The molecular structure of a deep eutectic solvent composed of urea and choline chloride.[27]

Results and Discussion

Polyampholyte Phase Behavior and Phase Inversion

We compared phase diagrams of DES/PA/water solutions with KBr/PA/water solutions, as KBr is shown to be an excellent salt to process polyelectrolytes.[21] The polyampholyte used in this study is produced from a feed solution containing 0.525 mole fraction of p-styrenesulfonic acid sodium salt and 0.475 mole fraction of 3-(methacryloylamino)propyl trimethylammonium chloride. This non-stoichiometric feed ratio has been shown to produce polyampholytes that are charged balanced.[33] It is thought that this charge balance is due the different reaction rates of the cationic and anionic monomers. Additionally, this composition has been shown to produce stable hydrogels that are strong and tough.[14] Thus, the molar concentration (M) for the polyampholyte refers to the overall repeat unit concentration of this polymer. As salt (DES or KBr in this case) is added, ion pairs within the polyampholyte are broken causing the polymer-rich phase to swell more. As with salt processing with traditional salts like KBr, the DES needs to be hydrated in order to dissolve, break the PA ion pairs, and allow the molecules to swell with water.[34,35] At sufficiently high salt concentrations, the PA fully dissolves and becomes a one-phase solution. Below the respective phase boundaries in Figure 2a and b, the DES/PA/water or KBr/PA/water solutions undergo

phase separation and are deemed two-phase, while above each boundary, the solutions are optically clear and thus one-phase. Qualitatively, the KBr boundary shape is in agreement with theoretical calculations that looked at the phase behavior of random polyelectrolyte sequences.[36] Additionally, the low KBr/PA concentration regime in this work is in agreement with Madinya *et al.* who used a transfer matrix method for theoretical calculations as well as experimental data to determine the phase boundary shape of polyampholytes in salt solutions.[37] In the DES case, molecular simulations in literature reveal that as water is added to a pure choline chloride/urea mixture, the urea molecules preferably hydrogen bond to water molecules, causing the diffusivity of the ions to increase and the viscosity of the solution to decrease.[30,38] This additional interplay between the water and DES may also be responsible for the irregular shape of the phase boundary for a PA concentration around 0.35 M. KBr can more easily break ion pairs due to its low solvation energy, resulting in the lower phase boundary compared to the DES in Figures 2a and b. Here, this urea/choline chloride deep eutectic solvent is used as it is one of the most readily available and well studied systems. A range of other deep eutectic solvents are also available and would change the position of the phase boundary based on various factors such as the strength of the ion pair.

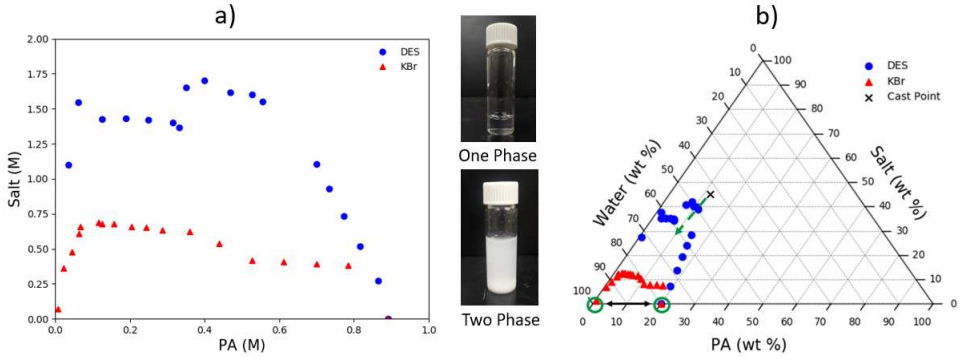

Figure 2: a) Phase boundaries in molar concentration for DES/PA/water mixtures in blue dots and KBr/PA/water compositions in red triangles. Samples that appear optically clear are considered one phase and above the phase boundary, while opaque solutions were deemed two phase and below the boundary. b) Ternary phase diagram in weight fraction of DES/PA/water solutions in blue dots and KBr/PA/water compositions in red triangles. The X represents the composition of Figure 3 before immersion in pure water.

In polyelectrolyte phase inversion, the coacervate is first separated from the dilute phase of the salt/polyelectrolyte/water solution, cast into a desired shape, and immediately immersed into pure water. Upon immersion, the salt ions are forced out of the film by an osmotic gradient causing the ionic bonds to no longer be doped and a rigid complex to be deposited. This phase inversion method has been previously used to rapidly fabricate porous membranes for filtration applications.[24] This concept can now be extended to the DES/PA/water systems using the phase diagrams in Figure 2a and b. Here, a solution of DES/PA/water with the composition of X in Figure 2b was spun coat onto a substrate and then immersed in a bath of pure water. The DES ions and water molecules then rapidly diffuse, moving the overall film composition into the two phase region, with the composition of the polymer-rich phase given by the phase boundary. As a result, the film is re-cast as a thin, smooth, homogeneous film as seen in Figure 3 a with a thickness of $\sim 3\mu m$. This thickness can further be controlled through varying the spin speed or composition and is discussed later in this manuscript. To compare to the traditional salt processing method from Sadman *et al.*[24], the same inversion technique using a KBr/PA/water solution was applied and the resulting film's cross-section shown in Figure 3 b. Qualitatively, these films look similar in terms of homogeneity and smoothness. Thus, deep eutectic solvents can be used in the place of traditional salts for immersion precipitation methods and other applications already demonstrated in literature using the polyelectrolyte/salt continuum.[23,24,39]

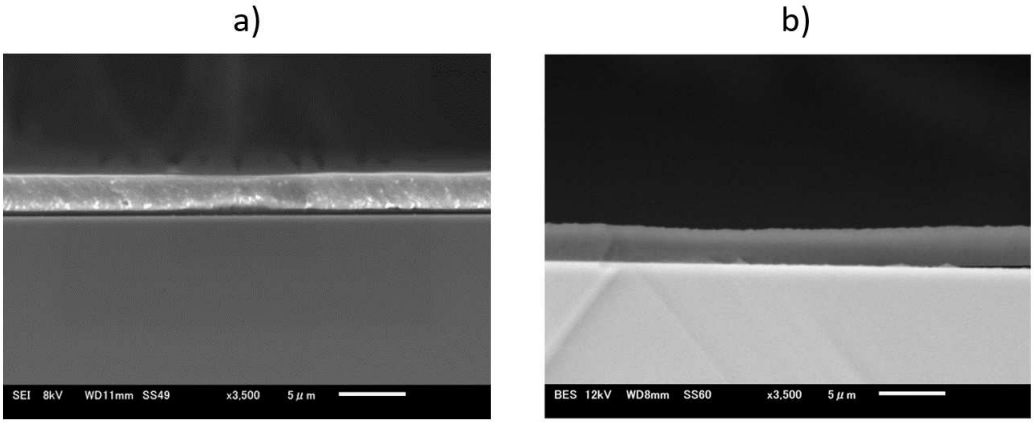

Figure 3: Cross-sectional scanning electron microscope images of a PA film after immersion of either a a) DES/PA/water solution (denoted as an X in Figure 2) or a b) KBr/PA/water solution in a bath of pure water. Due to the osmotic gradient upon submersion, both the DES and KBr are rapidly forced out of their respective mixtures causing similar smooth, thin, homogeneous PA films to be deposited on the substrate.

The Effect of Salt on Dry Film Morphology

The development of a polyelectrolyte/polyampholyte immersion precipitation process opens these systems to new applications, yet one critical challenge is the re-crystallization of salt in ambient environments. Such an effect is especially prevalent in thin film applications where the evaporation of water can take place on the order of seconds, causing the concentration of salt to increase beyond the solubility limit and disrupt the film morphology. To combat this effect, cast polyelectrolyte films are either rapidly quenched in water to form membranes or annealed in salt solutions for hours.[21,40] Additionally, membranes can be exposed to a humid atmosphere and high temperatures post quenching to reduce roughness in the material.[41] While valuable, these techniques introduce additional steps than can hinder the efficient processing of these materials at scale.

Table 1: Composition of DES/PA/water and KBr/PA/water solutions used to spin coat the films found in Figure 4.

Sample	Polyampholyte (wt%)	H_2O (wt%)	KBr (wt%)	DES(wt%)
DES	7.72(0.37M)	45.78	-	46.5(0.19M)
KBr	7.45(0.37M)	88.86	3.69(0.19M)	-

To investigate the stability of DES/PA/water films, 0.37 M PA was dissolved in aqueous solutions with 1.9 M of either DES or KBr. The respective weight fraction of these compositions are reported in Table 1. These separate films were then spun cast and left to dry for 12 hours in ambient conditions. Seconds after casting, visible KBr crystals formed causing significant roughness as shown in Figure 4a(i) and remained overnight as shown in Figure 4a(ii). Conversely after the initial spin coating, the DES/PA/water films remained transparent and smooth as seen in Figure 4b(i). Instead of recrystallizing as water evaporates, the DES forms the structure found in Figure 1b that prevents long range ordering and allows the counter ions to remain liquid-like at ambient conditions.[27,29] After the 12 hour exposure, the DES remained stable and smooth as shown in Figure 4b(ii). Moreover, following this extended time period, there is a low concentration of water in the film and thus the low freezing point of the DES prevents re-crystallization or disruption in the film morphology. From there, each film was then immersed in a bath of pure water for 1 hour to extract the DES or KBr via phase inversion as described by Sadman et al.[24] While Figure 4a(iii) shows the removal of the KBr, the film morphology is still compromised from the quenching process and is further evident in the optical microscopy shown in Figure 5a. For KBr/PA/water films, differences in local diffusion of the salt causes visible roughness to appear and disrupt the film. For DES/PA/water solutions, however, Figure 5b shows the smooth edge of the film from Figure 4b(iii). Here, the edge of the film is shown, as the surface of such a smooth film would appear dark under optical microscopy. Finally, optical profilometry over a 1.14 μm^2 area reveals an average surface roughness value, Ra, of 4.51 nm for the film cast from the DES/PA/water solution while the counterpart film cast from the KBr/PA/water solution has over two orders of magnitude more roughness with a Ra value of 310 nm. Thus, the non-volatility and salt-like behavior of the DES allows these polyampholytes to be fabricated in stable thin-film form without expensive or exotic processing conditions.

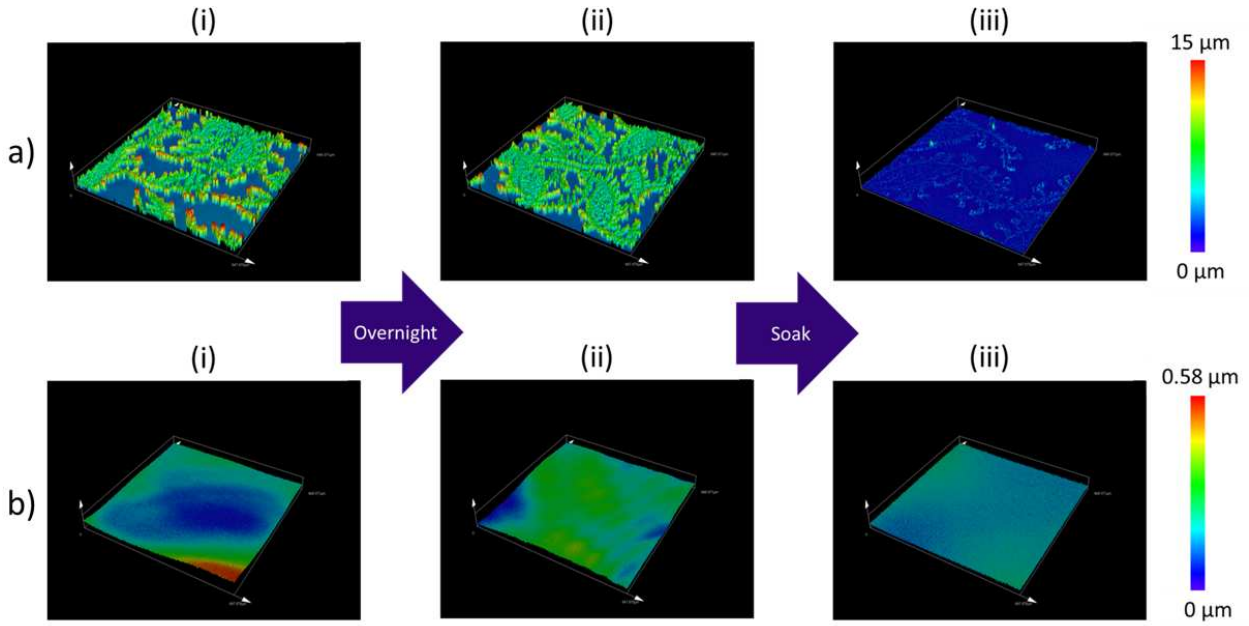

Figure 4: Surface roughness found for a) KBr/PA films for a film (i) after spin coating, (ii) after 12 hours in ambient conditions, and (iii) after immersion in water for an hour and drying. The same conditions were applied to DES/PA films for b) (i) - (iii)respectively.

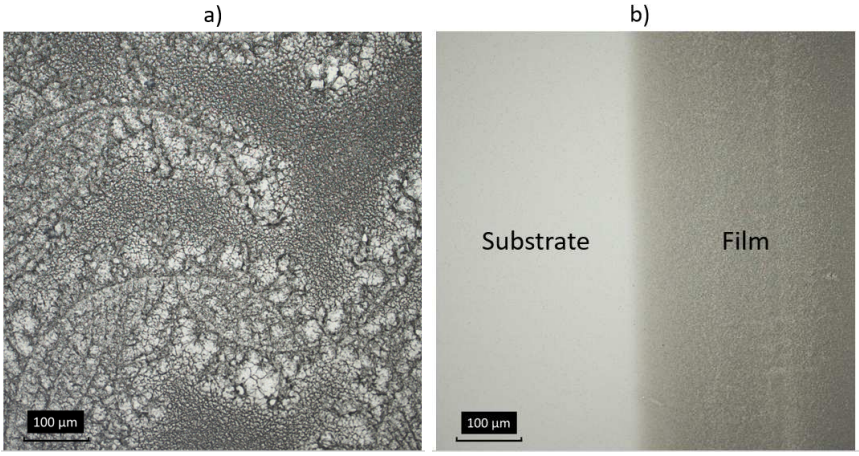

Figure 5: Top down optical microscope images of films cast from a) KBr/PA/water and b) DES/PA/water solutions after submersion in pure water to remove salt ions and recast the film.

Rheological Properties of Deep Eutectic Solvent/Polyampholyte Gels

In applications such as 3-D printing or injection molding, the rheological properties of the charged complexes would need to span a wide range of values, as first they would need to be liquid-like to be deposited on the desired surface, and then rapidly become rigid in order to deliver mechanical integrity.[42,43] The basic rheological features of these systems have been reviewed recently and are relatively well understood.[44–46] Wang et al. demonstrated that these polyelectrolyte complexes can move from a solid to viscoelastic liquid to a fully dilute system through the simple inclusion of salt ions.[22] Such a continuum allows these charged complexes to flow and be processed like traditional polymer/solvent mixtures into membranes[24], rods[23], and nanocomposites.[39]

Likewise, the rheological properties of the DES/PA/water and KBr/PA/water solutions were studied. The frequency dependent complex shear modulus can be fit using a purely viscous dash-pot in series with a power-law spring-pot element, yielding the following expression for G^*:[21,47]

$$\frac{G^*}{G^s} = \frac{(i\omega\tau)^\beta}{1+(i\omega\tau)^{\beta-1}}$$

The complex viscosity is then given as $\eta^* = \frac{G^*}{i\omega}$ and the zero shear viscosity, η_0 is equal to $G^s\tau$. Substituting for both G^* and G^S gives:

$$\frac{\eta^*}{\eta_0} = \frac{(i\omega\tau)^{\beta-1}}{1+(i\omega\tau)^{\beta-1}}$$

Here, η_0 and τ both scale with a_c. Thus, $\frac{\eta^*}{a_c}$vs ωa_c was plotted and fit in Figure 6a(i) and Figure 6b(i) for DES/PA/water and KBr/PA/water solutions respectively. Interestingly, Figure 6a(i) and a(ii) show that increasing the concentration of the DES actually increases the viscosity of the solution. Such a trend runs counter to similar KBr/PA/water rheological

curves in Figure 6b(i) and b(ii) as well as rheological measurements found in literature where increasing the salt concentration decreases the overall viscosity.[21,22,46]

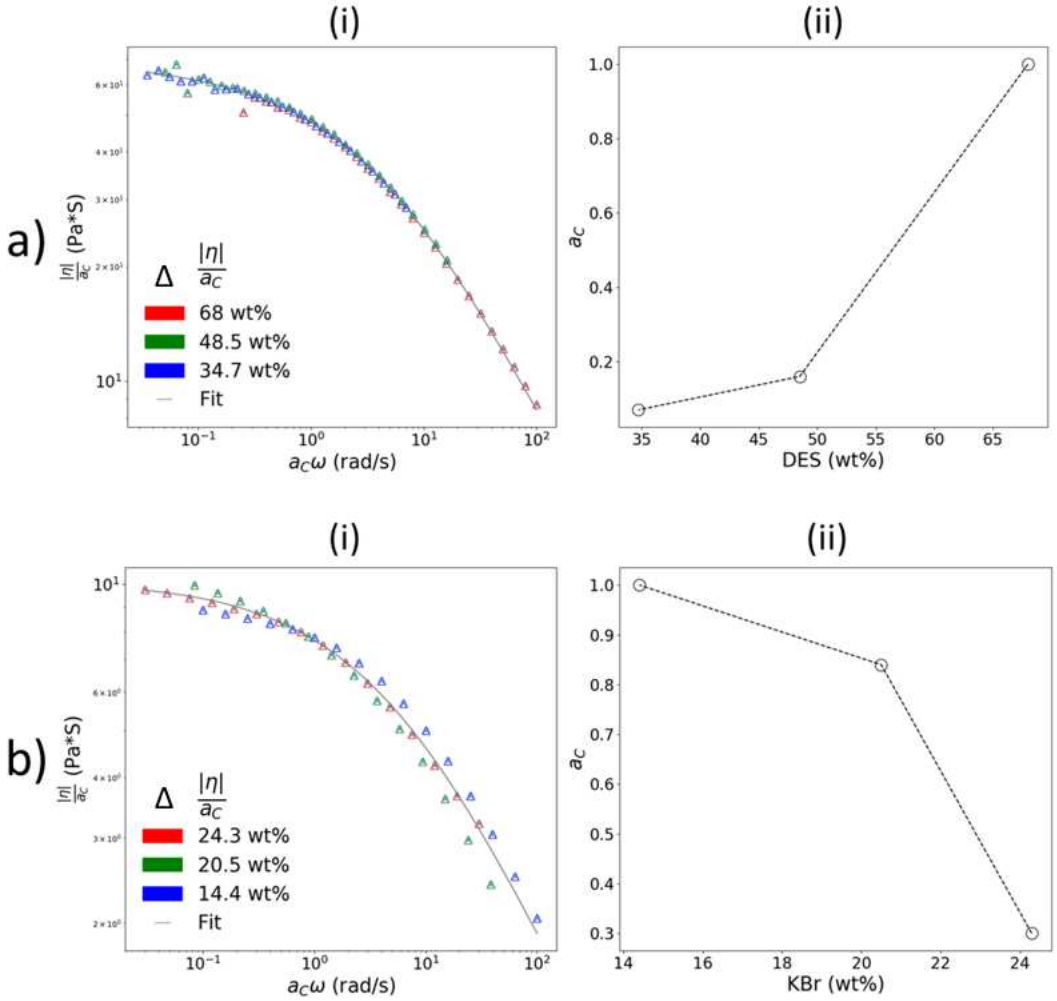

Figure 6: a) DES/PA/water and b) KBr/PA/water (i) viscosities normalized by the concentration dependent shift factors as well as (ii) the shift factors at each respective salt concentration. Each viscosity curve was fit using a viscous dash-pot in series with a power-law spring-pot element.[21,47] For the DES/PA/water solutions, the PA weight fraction is held constant at 27 wt% while for the KBr/PA/water solutions, the PA weight fraction is held constant at 12 wt%.

This result can be attributed to the composition dependence of the solvent viscosity. For the concentrations used in these experiments, the viscosity of the DES/water mixtures increases by nearly an order of magnitude in comparison to the value for pure water, as seen in the values taken from literature and presented in Table 2[32]. Indeed, when normalized

by these values, the relative viscosity in Figure 7 of the DES/PA/water solutions decreases with an increase in salt concentration following the same trend seen in the PA/KBr/water solutions and in literature.[22] The increase in DES concentration not only changes the rheological properties of the polyampholyte but also the solvent. This behavior is a departure from traditional behavior of salt/polyelectrolyte/water systems where the solvent viscosity is generally invariant to the addition of salt. These effects on the solvent viscosity provide a new tool to further tailor the rheological properties of these charged systems.

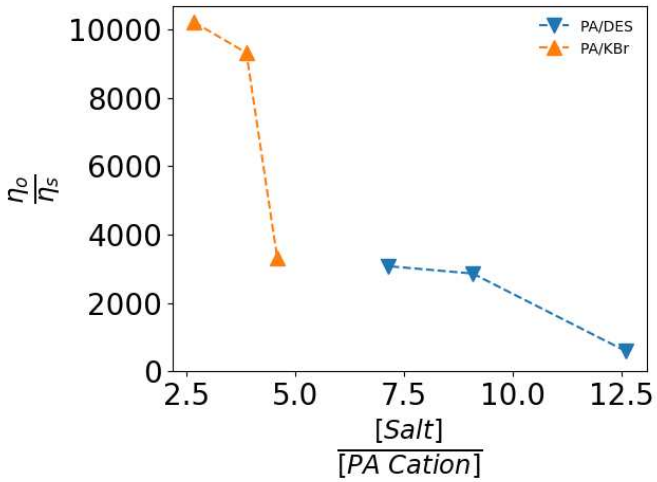

Figure 7: The zero shear viscosities (η_o) of the DES/PA/water and KBr/PA/water solutions were normalized by their respective solvent viscosities (η_s). Values for the DES/water viscosities at the different concentrations were taken from literature and presented in Table 2.[32]

Table 2: DES wt% in the DES/PA/water solutions and the corresponding DES viscosities.[32]

DES(wt%) (DES/PA/Water)	DES Viscosity (Pa-s)
68	0.092
48.5	0.0034
34.7	0.0013

This potential is illustrated in the schematic phase diagrams for the KBr/PA/water and DES/PA/water systems drawn in Figure 8a and b. In both cases, single phase solutions of KBr/PA/water and DES/PA/water are first cast in the processing window. Films are generally diluted along the dashed lines via immersion in a bath of pure water to recast the

polymer film.[24] In situations where this dilution is not immediate, water in the film will evaporate and the composition will move along the solid black arrow. For the KBr solution in Figure 8a, the composition will eventually move beyond the solubility limit of KBr causing the salt to re-crystallize and disrupt the film morphology. Thus, the processing window of the KBr/PA/water solution is confined by this solubility limit. For most traditional salts, this solubility line can shift depending on the ion pair, however, the processing window will still remained restricted below this limit. For the DES solution in Figure 8b, however, the DES does not re-crystallize due to its low freezing point allowing the film to remain stable at low water compositions. Moreover, because the viscosity of the DES is sensitive to water concentrations, one can still tailor rheological properties even at this low water regime. Thus, the stability of deep eutectic solvents expands the processing window of salt/charge molecule/water solutions into new and interesting compositions.

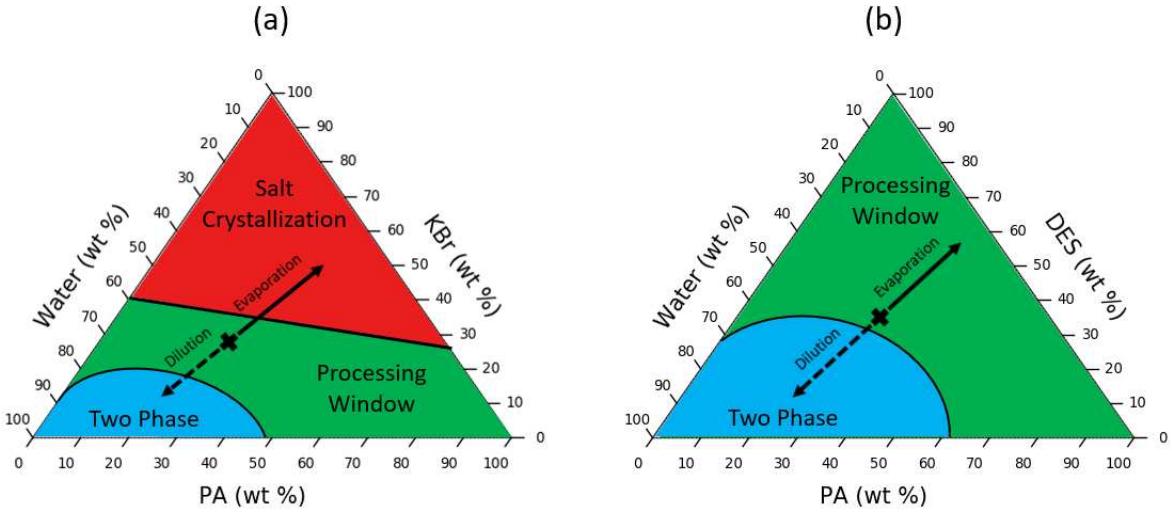

Figure 8: Generalized phase diagrams for a) KBr/PA/water and b) DES/PA/water solutions. The straight line in a) denotes the solubility limit of KBr under the assumption that the PA does not change this solubility. Films are initially cast at some point X and upon immersion, will move along the dashed line. If left exposed to ambient conditions, the water in the film will evaporate and move along the solid arrow line.

Processing Thin Polyampholyte Films

The ability to controllably deposit thin films (<100nm) of these PA hydrogels enables a variety of new applications. For example, while currently fabricated thick blocks of tough hydrogels are useful in fully replacing cartilage in the knee or hip, for some cases, it is advantageous to partially replace cartilage with hydrogel films of varying thicknesses.[48–50] Existing methodologies to fabricate thin film hydrogels for applications in drug delivery, anti-fouling coatings, and nanofluidics, however, utilize expensive and exotic processes such as plasma polymerization, polymer grafting, and e-beam radiation[51–53] For polyelectrolyte complexes on the other hand, the viscoelastic properties of the salt-polyelectrolyte continuum enable traditional thin-film processing methods such as spin coating, dip coating, and blade casting to be utilized.[24]

The film thickness obtained from these methods is strongly affected by the solution viscosity, which is controlled by solvent composition as discussed above, and also by the overall polymer concentration. To investigate this control, DES/PA/water solutions with different weight fractions of PA were spun at a constant spin speed, immersed in pure water to remove the DES, and subsequently recast into thin films. As the concentration of polymer decreased, the thickness of the resultant PA film also decreased, spanning over an order of magnitude from 1304 nm to 76 nm as seen in Figure 9. At each polymer concentration, the thickness can also be controlled by varying the spin speed.[54] Moreover, these DES/PA/water solutions can coat non-planer surfaces such as a mock hip joint through a simple dip coating procedure as seen in Figure 10a. Here, a joint with a surface area of roughly 28 cm^2 is first immersed in a DES/PA/water solution containing 35 wt% DES, 12 wt% PA, and 53 wt% H_2O. The coated joint can then be immersed in bath of pure water causing the DES to diffuse out of the coating as seen in Figure 10b and 10c. After only ~ 1 minute, the PA gel is redeposited on the complex surface shown in Figure 10d. In each method described, the stability of the DES allowed these films to be fabricated in ambient conditions while remaining in the large processing window described in Figure8b. As a result, these PA hydrogels are able to

be applied at the same length scales as previous thin-film hydrogel literature without any exotic, expensive, or time-consuming processing steps.

While these results have demonstrated that we can cast films over a wide range of thicknesses, testing the bulk mechanical properties of large-area thin films represents a significant challenge. Recently, custom thin film tensile testers have been developed which can test the mechanical response of thin films down to the 10's of nm scale.[55,56] In future work, we plan to make use of these techniques to compare the confinement effects of thin film hydrogels.

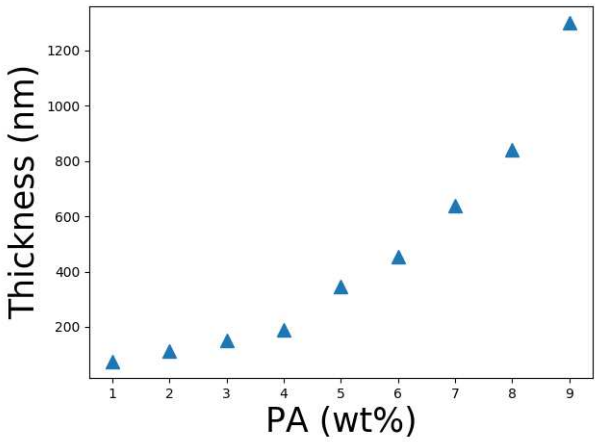

Figure 9: Thickness measurements of PA films from DES/PA/water solutions with different intial PA weight fractions. Each film was spun coat at 3000 rpm with an acceleration of 3000rpm/s for 30seconds.

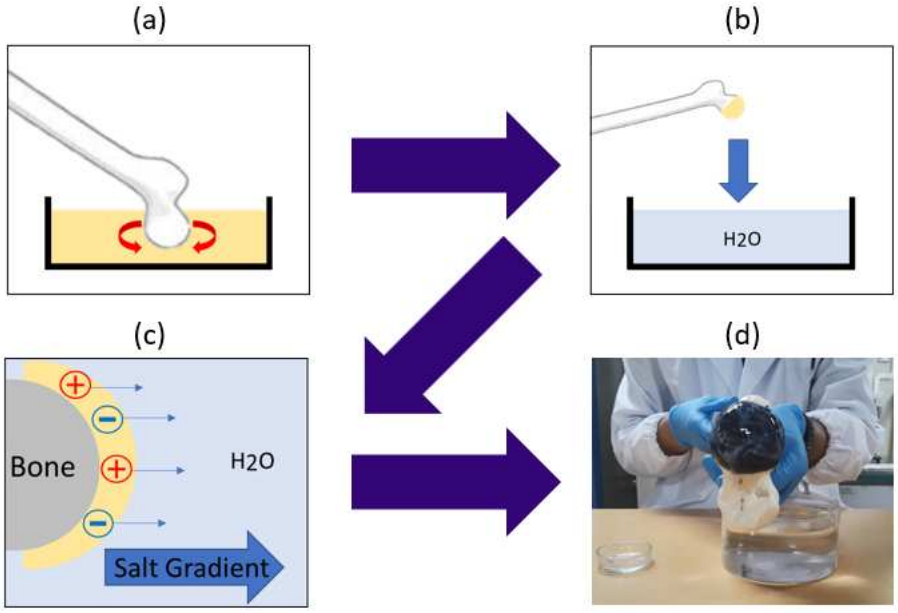

Figure 10: a) A mock hip joint is dipped in a viscoelastic solution of DES/PA/water at the same composition used in in table 1. b) The coated joint is immersed in a bath of pure water for ~1 minute. c) The osmotic gradient forces the DES ions to diffuse into the bath. d) A thin film is deposited on the complex surface of the hip joint.

Conclusion

In this study, we use an inert deep eutectic solvent composed of urea and choline chloride as a medium to process polyampholyte hydrogels from aqueous solutions into films as thin as ~70 nm. Ternary phase diagrams of DES/PA/water and KBr/PA/water were constructed to compare DES to traditional salt phase behavior. It was found that the DES is weaker at breaking ion pairs and thus has a higher composition phase boundary. The DES, however, has no solubility limit, allowing stable one phase solutions at concentrations where KBr would precipitate. We utilize this phase behavior to recast thin films of these polyampholyte hydrogels via immersion precipitation in a solution of pure water. Separate films of KBr/PA/water and DES/PA/water were cast and then left overnight in ambient conditions. As the water rapidly evaporated, the KBr re-crystallized and disrupted the film morphology. In contrast, the low freezing point and lack of vapor pressure of the DES allowed the

DES/PA/water films to remain stable, even overnight. Upon immersion in a bath of pure water, both the DES and KBr diffused into the surrounding environment. When developed through this process, the KBr/PA/water film had over two orders of magnitude more surface roughness than the DES film. Moreover, rheological experiments demonstrated that as the concentration of DES increased in the DES/PA/water system, the viscosity and shift factors actually increased. This relationship runs counter to the trend found in traditional coacervate-salt processing as well as KBr/PA/water processing. The relative viscosity of both the DES/PA/water and KBr/PA/water mixtures, however, both decreased with increasing the quantity of DES or KBr respectively. This trend is attributed to water impacting both the rheological properties of the the DES as well as the doping level of the PA.

The thickness of these PA hydrogels can be controlled by varying spin speed or polymer concentration. Films as thin as ~70 nm can be fabricated which is over an order of magnitude thinner than previous literature. Finally, this PA hydrogel can be coated onto complex surfaces through the use of a simple dip coating procedure. Leveraging the stability of DES when processing PA hydrogels is a step forward in realizing the full potential of these charged macromolecules in an efficient manner.

Experimental

Materials: P-styrenesulfonic acid sodium salt, 3-(methacryloylamino)propyl trimethylammonium chloride, and 2-oxoglutaric acid were purchased and used as is from Fujifilm Wako Chemicals. Potassium bromide (KBr), sodium chloride (NaCl), choline chloride, and urea were purchased from Sigma-Aldrich. Deionized water (conductivity $\approx 5\mu S/cm$) was used for making all solutions unless otherwise noted.

Polymerization of P(MPTC-co-NaSS) Polyampholyte: Polymerization of the polyampholyte (PA) follows the procedure outlined in literature.[9] In short, monomers of 3-(methacryloylamino)propyl trimethylammonium chloride (MPTC) and sodium 4-

styrenesulfonate (NaSS) monomers were mixed in an aqueous solution at a ratio of 0.95 M MPTC and 1.05 M NaSS for a total of 2 M. This ratio is found to be ideal for strong and tough gel formation.[14] Additionally, 0.5 NaCl and 0.1 mol% (relative to the total monomer molar concentration) 2-oxoglutaric acid initiator were added to the solution. The well mixed solution was then poured into a reaction vessel composed of two glass plates along with 4 mm spacing and placed in a nitrogen purged glove box. The mold was exposed to a 365 nm UV light for 8 hours. Upon removal from the plates, the PA hydrogel was immersed in a bath of water which was periodically changed for one week, in order to removed excess molecules and counter ions. This gel was then cut and freeze dried to remove moisture and form a dried powder.

Deep Eutectic Solvent and Phase Behavior: Urea and choline chloride were mixed at a 2 : 1 molar ratio and then stirred while the mixture was heated to 90°C for one hour. Upon cooling, the deep eutectic solvent (DES) remained a liquid that was stored in a desiccator for later use. To study the phase behavior, the PA was mixed into aqueous solutions at different weight fractions and then either DES or KBr was titrated into the respective solutions. At each titration step, the solution was deemed two phase if it was optically hazy or opaque and one phase if it was optically clear.

Surface Roughness Measurement and Imaging: Aqueous solutions of 0.37 M PA and 1.9 M of either KBr or DES were spun cast onto a 1 mm thick glass slide. The respective films were immediately imaged using an Olympus 3D laser confocal microscope. The films were then left on the bench top in ambient conditions for 12 hours and likewise imaged. Finally, the films were submerged in a bath of pure water for 1 hour and then dried using compressed air. Once dry, the films were again imaged and then the surface roughness was found using a Bruker Contour GT-K 3D Optical Microscope with an objective lens of 50. For the KBr/PA film roughness, the VSI mode was used while the PSI mode was used for the DES/PA/water films.

Rheometry: Rheological behaviors of DES/PA/water solutions were probed by an ARES

G2 rheometer using a stainless steel cone-plate geometry (50 mm diameter, 2°angle). Frequency sweeps were performed from 0.1 to 100 rad/s. A 1 % strain amplitude was used and confirmed to be in the linear viscoelastic regime by amplitude sweeps. Each experiment was carried out at 25°C. Once the polyampholyte solution was loaded into the cell, it was allowed to relax for 10 minutes. Water evaporation was mitigated by placing small troughs of water within the isolated cell. For the KBr/PA/water solutions, the rheological properties were found using an Anton-Paar MCR 302 rheometer with the same parameters used for the DES/PA/water solutions.

Thickness Measurements: DES/PA/water solutions were made using different weight fractions of PA. The solutions were then spun coat onto silicon chips using a WS-650MZ-23NPP spin coater at 3000 rpm with a 3000 rpm/s acceleration for 30seconds. After spin coating, the film was immersed in a bath of pure water for 20minutes to remove the DES and re-cast the PA film. Each film was notched using a razor blade and the thickness was found using a Veeco Dektak 150 surface profiler.

Acknowledgments

David Delgado thanks Global Station for Soft Matter, Global Institution for Collaborative Research, Hokkaido University for financial support of his stay at Hokkaido University. This work was supported by the National Science Foundation (NSF DMR-1710491) and made use of the MatCI Facility which receives support from the MRSEC Program (NSF DMR-1720139) of the Materials Research Center at Northwestern University. This work made use of the EPIC facility of Northwestern University's NUANCE Center, which has received support from the Soft and Hybrid Nanotechnology Experimental (SHyNE) Resource (NSF ECCS-1542205); the International Institute for Nanotechnology (IIN); the Keck Foundation; and the State of Illinois, through the IIN. This research was also supported by Grant-in-Aid for Scientific Research No. JP17H06144 from the Japan Society for the Promotion of

Science (JSPS). The Institute for Chemical Reaction Design and Discovery (ICReDD) was established by World Premier International Research Initiative (WPI), MEXT, Japan.

References

(1) Banerjee, H.; Ren, H. Optimizing Double-Network Hydrogel for Biomedical Soft Robots. *Soft Robotics* **2017**, *4*, 191–201, DOI: 10.1089/soro.2016.0059.

(2) Zhang, X.; Sheng, N.; Wang, L.; Tan, Y.; Liu, C.; Xia, Y.; Nie, Z.; Sui, K. Supramolecular Nanofibrillar Hydrogels as Highly Stretchable, Elastic and Sensitive Ionic Sensors. *Materials Horizons* **2019**, *6*, 326–333, DOI: 10.1039/C8MH01188E.

(3) W. Ooi, H.; Hafeez, S.; van Blitterswijk, C. A.; Moroni, L.; B. Baker, M. Hydrogels That Listen to Cells: A Review of Cell-Responsive Strategies in Biomaterial Design for Tissue Regeneration. *Materials Horizons* **2017**, *4*, 1020–1040, DOI: 10.1039/C7MH00373K.

(4) Haque, M. A.; Kurokawa, T.; Gong, J. P. Super Tough Double Network Hydrogels and Their Application as Biomaterials. *Polymer* **2012**, *53*, 1805–1822, DOI: 10.1016/j.polymer.2012.03.013.

(5) Creton, C. 50th Anniversary Perspective: Networks and Gels: Soft but Dynamic and Tough. *Macromolecules* **2017**, *50*, 8297–8316, DOI: 10.1021/acs.macromol.7b01698.

(6) Yasuda, K.; Ping Gong, J.; Katsuyama, Y.; Nakayama, A.; Tanabe, Y.; Kondo, E.; Ueno, M.; Osada, Y. Biomechanical Properties of High-Toughness Double Network Hydrogels. *Biomaterials* **2005**, *26*, 4468–4475, DOI: 10.1016/j.biomaterials.2004.11.021.

(7) Ping Gong, J. Why Are Double Network Hydrogels so Tough? *Soft Matter* **2010**, *6*, 2583–2590, DOI: 10.1039/B924290B.

(8) Gong, J. P.; Katsuyama, Y.; Kurokawa, T.; Osada, Y. Double-Network Hydrogels with Extremely High Mechanical Strength. *Advanced Materials* **2003**, *15*, 1155–1158, DOI: 10.1002/adma.200304907.

(9) Luo, F.; Sun, T. L.; Nakajima, T.; King, D. R.; Kurokawa, T.; Zhao, Y.; Ihsan, A. B.; Li, X.; Guo, H.; Gong, J. P. Strong and Tough Polyion-Complex Hydrogels from Oppositely Charged Polyelectrolytes: A Comparative Study with Polyampholyte Hydrogels. *Macromolecules* **2016**, *49*, 2750–2760, DOI: 10.1021/acs.macromol.6b00235.

(10) Ihsan, A. B.; Sun, T. L.; Kurokawa, T.; Karobi, S. N.; Nakajima, T.; Nonoyama, T.; Roy, C. K.; Luo, F.; Gong, J. P. Self-Healing Behaviors of Tough Polyampholyte Hydrogels. *Macromolecules* **2016**, *49*, 4245–4252, DOI: 10.1021/acs.macromol.6b00437.

(11) Mayumi, K.; Guo, J.; Narita, T.; Hui, C. Y.; Creton, C. Fracture of Dual Crosslink Gels with Permanent and Transient Crosslinks. *Extreme Mechanics Letters* **2016**, *6*, 52–59, DOI: 10.1016/j.eml.2015.12.002.

(12) Narita, T.; Mayumi, K.; Ducouret, G.; Hébraud, P. Viscoelastic Properties of Poly(Vinyl Alcohol) Hydrogels Having Permanent and Transient Cross-Links Studied by Microrheology, Classical Rheometry, and Dynamic Light Scattering. *Macromolecules* **2013**, *46*, 4174–4183, DOI: 10.1021/ma400600f.

(13) Sun, J.-Y.; Zhao, X.; Illeperuma, W. R. K.; Chaudhuri, O.; Oh, K. H.; Mooney, D. J.; Vlassak, J. J.; Suo, Z. Highly Stretchable and Tough Hydrogels. *Nature* **2012**, *489*, 133–136, DOI: 10.1038/nature11409.

(14) Sun, T. L.; Kurokawa, T.; Kuroda, S.; Ihsan, A. B.; Akasaki, T.; Sato, K.; Haque, M. A.; Nakajima, T.; Gong, J. P. Physical Hydrogels Composed of Polyampholytes Demonstrate High Toughness and Viscoelasticity. *Nature Materials* **2013**, *12*, 932–937, DOI: 10.1038/nmat3713.

(15) Cui, K.; Ye, Y. N.; Sun, T. L.; Chen, L.; Li, X.; Kurokawa, T.; Nakajima, T.; Nonoyama, T.; Gong, J. P. Effect of Structure Heterogeneity on Mechanical Performance of Physical Polyampholytes Hydrogels. *Macromolecules* **2019**, *52*, 7369–7378, DOI: 10.1021/acs.macromol.9b01676.

(16) Ye, Y. N.; Frauenlob, M.; Wang, L.; Tsuda, M.; Sun, T. L.; Cui, K.; Takahashi, R.; Zhang, H. J.; Nakajima, T.; Nonoyama, T.; Kurokawa, T.; Tanaka, S.; Gong, J. P. Tough and Self-Recoverable Thin Hydrogel Membranes for Biological Applications. *Advanced Functional Materials 0*, 1801489, DOI: 10.1002/adfm.201801489.

(17) Liang, S.; Yu, Q. M.; Yin, H.; Wu, Z. L.; Kurokawa, T.; Gong, J. P. Ultrathin Tough Double Network Hydrogels Showing Adjustable Muscle-like Isometric Force Generation Triggered by Solvent. *Chem. Commun.* **2009**, 7518–7520, DOI: 10.1039/B916581A.

(18) Hu, J.; Hiwatashi, K.; Kurokawa, T.; Liang, S. M.; Wu, Z. L.; Gong, J. P. Microgel-Reinforced Hydrogel Films with High Mechanical Strength and Their Visible Mesoscale Fracture Structure. *Macromolecules* **2011**, *44*, 7775–7781, DOI: 10.1021/ma2016248.

(19) Zhang, H. J.; Sun, T. L.; Zhang, A. K.; Ikura, Y.; Nakajima, T.; Nonoyama, T.; Kurokawa, T.; Ito, O.; Ishitobi, H.; Gong, J. P. Tough Physical Double-Network Hydrogels Based on Amphiphilic Triblock Copolymers. *Advanced Materials* **2016**, *28*, 4884–4890, DOI: 10.1002/adma.201600466.

(20) Liu, Y.; Momani, B.; Winter, H. H.; Perry, S. L. Rheological Characterization of Liquid-to-Solid Transitions in Bulk Polyelectrolyte Complexes. *Soft Matter* **2017**, *13*, 7332–7340, DOI: 10.1039/C7SM01285C.

(21) Sadman, K.; Wang, Q.; Chen, Y.; Keshavarz, B.; Jiang, Z.; Shull, K. R. Influence of Hydrophobicity on Polyelectrolyte Complexation. *Macromolecules* **2017**, *50*, 9417–9426, DOI: 10.1021/acs.macromol.7b02031.

(22) Wang, Q.; Schlenoff, J. B. The Polyelectrolyte Complex/Coacervate Continuum. *Macromolecules* **2014**, *47*, 3108–3116, DOI: 10.1021/ma500500q.

(23) Shamoun, R. F.; Reisch, A.; Schlenoff, J. B. Extruded Saloplastic Polyelectrolyte Complexes. *Advanced Functional Materials* **2012**, *22*, 1923–1931, DOI: 10.1002/adfm.201102787.

(24) Sadman, K.; Delgado, D. E.; Won, Y.; Wang, Q.; Gray, K. A.; Shull, K. R. Versatile and High-Throughput Polyelectrolyte Complex Membranes via Phase Inversion. *ACS Appl. Mater. Interfaces* **2019**, *11*, 16018–16026, DOI: 10.1021/acsami.9b02115.

(25) Zhao, D.; Liao, Y.; Zhang, Z. Toxicity of Ionic Liquids. *CLEAN – Soil, Air, Water* **2007**, *35*, 42–48, DOI: 10.1002/clen.200600015.

(26) Cao, L.; Zhu, P.; Zhao, Y.; Zhao, J. Using Machine Learning and Quantum Chemistry Descriptors to Predict the Toxicity of Ionic Liquids. *Journal of Hazardous Materials* **2018**, *352*, 17–26, DOI: 10.1016/j.jhazmat.2018.03.025.

(27) Ashworth, C. R.; Matthews, R. P.; Welton, T.; Hunt, P. A. Doubly Ionic Hydrogen Bond Interactions within the Choline Chloride–Urea Deep Eutectic Solvent. *Physical Chemistry Chemical Physics* **2016**, *18*, 18145–18160, DOI: 10.1039/C6CP02815B.

(28) Tang, B.; Row, K. H. Recent Developments in Deep Eutectic Solvents in Chemical Sciences. *Monatsh Chem* **2013**, *144*, 1427–1454, DOI: 10.1007/s00706-013-1050-3.

(29) Abbott, A. P.; Capper, G.; Davies, D. L.; Rasheed, R. K.; Tambyrajah, V. Novel Solvent Properties of Choline Chloride/Urea Mixtures. *Chem. Commun.* **2003**, 70–71, DOI: 10.1039/B210714G.

(30) Fetisov, E. O.; Harwood, D. B.; Kuo, I.-F. W.; Warrag, S. E. E.; Kroon, M. C.; Peters, C. J.; Siepmann, J. I. First-Principles Molecular Dynamics Study of a Deep Eu-

tectic Solvent: Choline Chloride/Urea and Its Mixture with Water. *J. Phys. Chem. B* **2018**, *122*, 1245–1254, DOI: 10.1021/acs.jpcb.7b10422.

(31) Agieienko, V.; Buchner, R. Densities, Viscosities, and Electrical Conductivities of Pure Anhydrous Reline and Its Mixtures with Water in the Temperature Range (293.15 to 338.15) K. *J. Chem. Eng. Data* **2019**, DOI: 10.1021/acs.jced.9b00145.

(32) Yadav, A.; Pandey, S. Densities and Viscosities of (Choline Chloride + Urea) Deep Eutectic Solvent and Its Aqueous Mixtures in the Temperature Range 293.15 K to 363.15 K. *J. Chem. Eng. Data* **2014**, *59*, 2221–2229, DOI: 10.1021/je5001796.

(33) Cui, K.; Ye, Y. N.; Sun, T. L.; Yu, C.; Li, X.; Kurokawa, T.; Gong, J. P. Phase Separation Behavior in Tough and Self-Healing Polyampholyte Hydrogels. *Macromolecules* **2020**, *53*, 5116–5126, DOI: 10.1021/acs.macromol.0c00577.

(34) Zhang, B.; Hoagland, D. A.; Su, Z. Ionic Liquids as Plasticizers for Polyelectrolyte Complexes. *J. Phys. Chem. B* **2015**, *119*, 3603–3607, DOI: 10.1021/jp5128354.

(35) Parveen, N.; Schönhoff, M. Swelling and Stability of Polyelectrolyte Multilayers in Ionic Liquid Solutions. *Macromolecules* **2013**, *46*, 7880–7888, DOI: 10.1021/ma401625r.

(36) Rumyantsev, A. M.; Jackson, N. E.; Yu, B.; Ting, J. M.; Chen, W.; Tirrell, M. V.; de Pablo, J. J. Controlling Complex Coacervation via Random Polyelectrolyte Sequences. *ACS Macro Lett.* **2019**, 1296–1302, DOI: 10.1021/acsmacrolett.9b00494.

(37) Madinya, J. J.; Chang, L.-W.; Perry, S. L.; Sing, C. E. Sequence-Dependent Self-Coacervation in High Charge-Density Polyampholytes. *Mol. Syst. Des. Eng.* **2019**, DOI: 10.1039/C9ME00074G.

(38) Shah, D.; Mjalli, F. S. Effect of Water on the Thermo-Physical Properties of Reline: An Experimental and Molecular Simulation Based Approach. *Phys. Chem. Chem. Phys.* **2014**, *16*, 23900–23907, DOI: 10.1039/C4CP02600D.

(39) Fu, J.; Wang, Q.; Schlenoff, J. B. Extruded Superparamagnetic Saloplastic Polyelectrolyte Nanocomposites. *ACS Appl. Mater. Interfaces* **2015**, *7*, 895–901, DOI: 10.1021/am5074694.

(40) Kelly, K. D.; Schlenoff, J. B. Spin-Coated Polyelectrolyte Coacervate Films. *ACS Appl. Mater. Interfaces* **2015**, *7*, 13980–13986, DOI: 10.1021/acsami.5b02988.

(41) Kurtz, I. S.; Sui, S.; Hao, X.; Huang, M.; Perry, S. L.; Schiffman, J. D. Bacteria-Resistant, Transparent, Free-Standing Films Prepared from Complex Coacervates. *ACS Appl. Bio Mater.* **2019**, *2*, 3926–3933, DOI: 10.1021/acsabm.9b00502.

(42) Ramirez Caballero, S. S.; Saiz, E.; Montembault, A.; Tadier, S.; Maire, E.; David, L.; Delair, T.; Grémillard, L. 3-D Printing of Chitosan-Calcium Phosphate Inks: Rheology, Interactions and Characterization. *J Mater Sci: Mater Med* **2018**, *30*, 6, DOI: 10.1007/s10856-018-6201-y.

(43) Shojaeiarani, J.; Bajwa, D. S.; Stark, N. M.; Bajwa, S. G. Rheological Properties of Cellulose Nanocrystals Engineered Polylactic Acid Nanocomposites. *Composites Part B: Engineering* **2019**, *161*, 483–489, DOI: 10.1016/j.compositesb.2018.12.128.

(44) Hyun, K.; Wilhelm, M.; Klein, C. O.; Cho, K. S.; Nam, J. G.; Ahn, K. H.; Lee, S. J.; Ewoldt, R. H.; McKinley, G. H. A Review of Nonlinear Oscillatory Shear Tests: Analysis and Application of Large Amplitude Oscillatory Shear (LAOS). *Progress in Polymer Science* **2011**, *36*, 1697–1753, DOI: 10.1016/j.progpolymsci.2011.02.002.

(45) Liu, Y.; Winter, H. H.; Perry, S. L. Linear Viscoelasticity of Complex Coacervates. *Advances in Colloid and Interface Science* **2017**, *239*, 46–60, DOI: 10.1016/j.cis.2016.08.010.

(46) Marciel, A. B.; Srivastava, S.; V. Tirrell, M. Structure and Rheology of Polyelectrolyte Complex Coacervates. *Soft Matter* **2018**, *14*, 2454–2464, DOI: 10.1039/C7SM02041D.

(47) Jaishankar, A.; McKinley, G. H. Power-Law Rheology in the Bulk and at the Interface: Quasi-Properties and Fractional Constitutive Equations. *Proc. R. Soc. A* **2013**, *469*, 20120284, DOI: 10.1098/rspa.2012.0284.

(48) Yuk, H.; Zhang, T.; Parada, G. A.; Liu, X.; Zhao, X. Skin-Inspired Hydrogel–Elastomer Hybrids with Robust Interfaces and Functional Microstructures. *Nature Communications* **2016**, *7*, 12028, DOI: 10.1038/ncomms12028.

(49) Zhang, Y. S.; Khademhosseini, A. Advances in Engineering Hydrogels. *Science* **2017**, *356*, DOI: 10.1126/science.aaf3627.

(50) Takahashi, R.; Shimano, K.; Okazaki, H.; Kurokawa, T.; Nakajima, T.; Nonoyama, T.; King, D. R.; Gong, J. P. Double Network Gels: Tough Particle-Based Double Network Hydrogels for Functional Solid Surface Coatings (Adv. Mater. Interfaces 23/2018). *Advanced Materials Interfaces* **2018**, *5*, 1870118, DOI: 10.1002/admi.201870118.

(51) Bhattacharyya, D.; Pillai, K.; Chyan, O. M. R.; Tang, L.; Timmons, R. B. A New Class of Thin Film Hydrogels Produced by Plasma Polymerization. *Chem. Mater.* **2007**, *19*, 2222–2228, DOI: 10.1021/cm0630688.

(52) Zhao, Y.-F.; Zhu, L.-P.; Yi, Z.; Zhu, B.-K.; Xu, Y.-Y. Zwitterionic Hydrogel Thin Films as Antifouling Surface Layers of Polyethersulfone Ultrafiltration Membranes Anchored via Reactive Copolymer Additive. *Journal of Membrane Science* **2014**, *470*, 148–158, DOI: 10.1016/j.memsci.2014.07.023.

(53) Tirumala, V. R.; Divan, R.; Ocola, L. E.; Mancini, D. C. Direct-Write e-Beam Patterning of Stimuli-Responsive Hydrogel Nanostructures. *Journal of Vacuum Science & Technology B: Microelectronics and Nanometer Structures Processing, Measurement, and Phenomena* **2005**, *23*, 3124, DOI: 10.1116/1.2062649.

(54) Hall, D. B.; Underhill, P.; Torkelson, J. M. Spin Coating of Thin and Ultra-

thin Polymer Films. *Polymer Engineering & Science* **1998**, *38*, 2039–2045, DOI: 10.1002/pen.10373.

(55) Liu, Y.; Chen, Y.-C.; Hutchens, S.; Lawrence, J.; Emrick, T.; Crosby, A. J. Directly Measuring the Complete Stress–Strain Response of Ultrathin Polymer Films. *Macromolecules* **2015**, *48*, 6534–6540, DOI: 10.1021/acs.macromol.5b01473.

(56) Laprade, E. J.; Liaw, C.-Y.; Jiang, Z.; Shull, K. R. Mechanical and Microstructural Characterization of Sulfonated Pentablock Copolymer Membranes. *Journal of Polymer Science Part B: Polymer Physics* **2015**, *53*, 39–47, DOI: 10.1002/polb.23623.